

Quantitatively Analyzing Metathesis Catalyst Activity and Structural Features in Silica-Supported Tungsten Imido–Alkylidene Complexes

Victor Mougel,^{†,||} Celine B. Santiago,^{‡,||} Pavel A. Zhizhko,^{†,||,⊥} Elizabeth N. Bess,[‡] Jenő Varga,[§] Georg Frater,[§] Matthew S. Sigman,^{*,‡} and Christophe Copéret^{*,†}

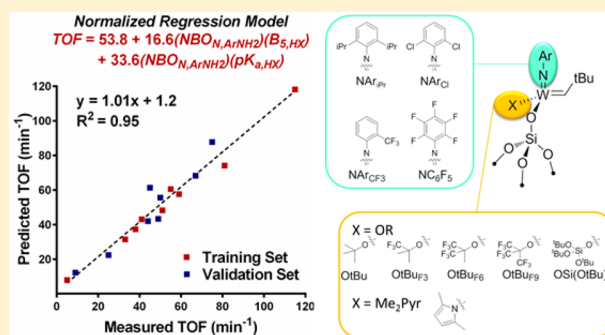
[†]Department of Chemistry and Applied Biosciences, ETH Zürich, Vladimir Prelog Weg 2, 8093 Zürich, Switzerland

[‡]Department of Chemistry, University of Utah, 315 South 1400 East, Salt Lake City, Utah 84112, United States

[§]XiMo Hungary, Zahony u. 7 H-1031 Budapest, Hungary

Supporting Information

ABSTRACT: A broad series of fully characterized, well-defined silica-supported W metathesis catalysts with the general formula $[(\equiv\text{SiO})\text{W}(=\text{NAr})(=\text{CHCMe}_2\text{R})(\text{X})]$ (Ar = 2,6-*i*Pr₂C₆H₃ (Ar_{iPr}), 2,6-Cl₂C₆H₃ (Ar_{Cl}), 2-CF₃C₆H₄ (Ar_{CF3}), and C₆F₅ (Ar_{F5}); X = OC(CF₃)₃ (OtBu_{F9}), OCMc(CF₃)₂ (OtBu_{F6}), OtBu, OSi(OtBu)₃, 2,5-dimethylpyrrolyl (Me₂Pyr) and R = Me or Ph) was prepared by grafting bis-X substituted complexes $[\text{W}(\text{NAr})(=\text{CHCMe}_2\text{R})(\text{X})_2]$ on silica partially dehydroxylated at 700 °C (SiO₂₋₍₇₀₀₎), and their activity was evaluated with the goal to obtain detailed structure–activity relationships. Quantitative influence of the ligand set on the activity (turnover frequency, TOF) in self-metathesis of *cis*-4-nonene was investigated using multivariate linear regression analysis tools. The TOF of these catalysts (activity) can be well predicted from simple steric and electronic parameters of the parent protonated ligands; it is described by the mutual contribution of the NBO charge of the nitrogen or the IR intensity of the symmetric N–H stretch of the ArNH₂, corresponding to the imido ligand, together with the Sterimol B₅ and pK_a of HX, representing the X ligand. This quantitative and predictive structure–activity relationship analysis of well-defined heterogeneous catalysts shows that high activity is associated with the combination of X and NAr ligands of opposite electronic character and paves the way toward rational development of metathesis catalysts.



INTRODUCTION

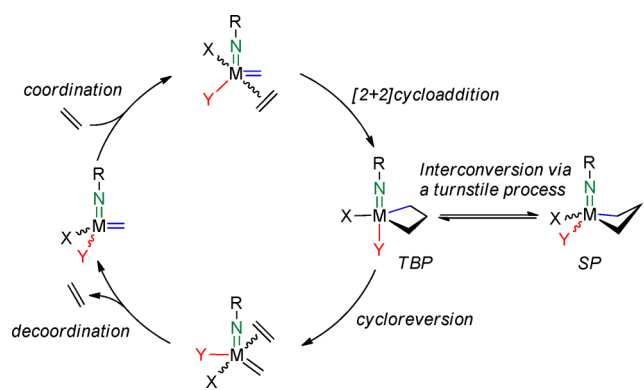
Over the last 50 years, olefin metathesis has transformed the way in which a diverse array of compounds, ranging from petrochemicals to advanced pharmaceuticals to polymers, can be efficiently prepared.¹ A pivotal point in the development of these transformations came through the work of Y. Chauvin, who demonstrated that alkylidenes and metallacyclobutanes were key reaction intermediates in the metathesis catalytic cycle.² This pioneering work led to the design of now well-known molecularly defined catalysts, based on either d⁰ (Mo, W and Re) or d⁶ (Ru) transition-metal alkylidene complexes.^{2,3} This mechanism has also influenced the latest development of heterogeneous metathesis catalysts having well-defined metal sites whose performances can now exceed their homogeneous counterparts.⁴ Computational investigations have also provided insights allowing for tremendous advances in the understanding of active site structure and reactivity of metathesis catalysts.^{5,6} For the broad class of d⁰ group 6–7 homogeneous and heterogeneous catalysts, the overall performance results from the combination of numerous factors acting in parallel and affecting both activity and stability.^{4a,b,d–f,h–k,5,7} These include (i) the barriers for olefin coordination and decoordination, (ii) the relative stabilities and different behavior of trigonal

bipyramidal (TBP) and square planar (SP) metallacycle intermediates, and (iii) the occurrence of several simultaneous deactivation pathways, such as dimerization of alkylidene species or β-hydride elimination of metallacycles, as well as catalyst poisoning by impurities (Scheme 1).

Despite these studies, the ligand effects and structural factors that influence the catalytic activity still remain unclear. For instance, it has been demonstrated that for d⁰ high-oxidation state catalysts of the general formula (X)(Y)M(E)(=CHR) [X, Y = anionic ligands and ME = Mo/W=NR or Re≡CR], the dissymmetry at the metal center (X ≠ Y) is key for high activity because it facilitates coordination/decoordination of the olefins and also destabilizes the most stable metallacyclobutane intermediates.^{5c,g} This model clearly explains the high activity of both silica-supported^{4d,h–k} and MAP catalysts.^{3j,8} Yet, it has also been revealed that having two strong electron withdrawing anionic ligands (fluorinated phenoxy, alkoxy, and/or siloxy) also leads to very active catalysts, indicating that other factors are important to obtain highly active catalysts.^{4j,9} Therefore,

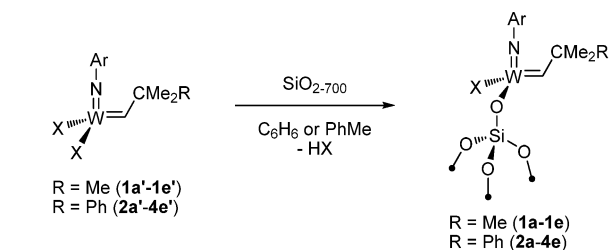
Received: March 31, 2015

Published: May 4, 2015

Scheme 1. Reaction Pathway Proposed for d⁰ Metal Alkene Metathesis Catalysts

there is a critical need to better understand and determine the origin of activity in this general catalyst family.

Here, we have engaged in a systematic investigation of catalyst structural properties that govern catalytic activity for a series of supported well-defined catalysts of the general formula $(\equiv\text{SiO})\text{W}(=\text{NAr})(=\text{CHCMe}_2\text{R})\text{X}$, bearing various arylimido groups (NAr), namely 2,6-*i*Pr₂C₆H₃ (NAr_{*i*Pr}), 2,6-Cl₂C₆H₃ (NAr_{Cl}), 2-CF₃C₆H₄ (NAr_{CF₃}), C₆F₅ (NAr_{F₅}), and anionic X ligands (X = OC(CF₃)₃ (OtBu_{F₉}), OCMe(CF₃)₂ (OtBu_{F₆}), OtBu, OSi(OtBu)₃, 2,5-dimethylpyrrolyl (Me₂Pyr)), as presented in Scheme 2. To accomplish this, we have utilized

Scheme 2. Preparation of Well-Defined Silica-Supported Tungsten Imido–Alkylidene Catalysts^a

	NAr _{<i>i</i>Pr}	NAr _{Cl}	NAr _{CF₃}	NAr _{F₅}
X				
	1a	2a	3a	4a
	1b	2b	3b	4b
	1c	2c	3c	4c
	1d	2d	3d	4d
	1e	2e	3e	4e

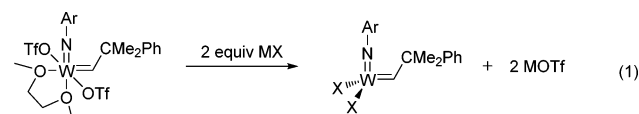
^aDesignations of molecular precursors are noted with a prime (').

multivariate linear regression analysis tools, which allow identification of discrete molecular features that quantitatively describe turnover frequency (TOF). The results of this investigation are reported and point to the interplay between the X and NAr ligands in directing the activity of the catalyst as evaluated by TOF. In particular, high activity is associated with the combination of X and NAr ligands of opposing electronic character (one electron withdrawing and the other electron donating), which is modulated by the sterics of the X ligand.

This can be readily quantified by parameters that measure the pK_a and Sterimol B₅ values of X and the NBO charge on N of the parent organic molecules HX and ArNH₂, respectively.

RESULTS AND DISCUSSION

Synthesis of the Molecular Precursors. Complexes of the NAr_{*i*Pr} series (**1a'**–**1e'**) were prepared as previously described.^{4j,10} Similarly, a new series of complexes bearing NAr_{Cl},¹¹ NAr_{CF₃}, and NAr_{F₅}¹² imido ligands were prepared by salt metathesis of the corresponding bis(triflate) complexes with 2 equiv of Li or K alkoxide, siloxide, or pyrrolide (eq 1).



MX = LiOtBuF₉ (**2a'**–**4a'**), LiOtBuF₆ (**2b'**–**4b'**), KOSi(OtBu)₃ (**2c'**–**3c'**), Me₂PyrLi (**2e'**–**4e'**)

We noted that the alkoxide and siloxide complexes bearing electron-withdrawing imido ligands display lower stability than their Ar_{*i*Pr} analogues. This feature is especially noteworthy in the Ar_{F₅} series, preventing the synthesis of complexes **4c'** and **4d'**, which were observed by NMR but could not be isolated due to their instability (see Supporting Information for details).

Preparation of Supported Complexes. The supported catalysts were prepared by contacting a benzene suspension of silica partially dehydroxylated at 700 °C (SiO₂₋₍₇₀₀₎, 0.26 mmol SiOH/g) with a benzene solution of a molecular precursor (1.05 equiv with respect to the total amount of surface silanol groups in the silica sample) at ambient temperature for 12 h. For the temperature sensitive NAr_{F₅} compounds **4a'**–**4b'**, grafting was performed in toluene, and the solution of molecular precursor was precooled to –40 °C before addition. Contact time in these cases was reduced to 30 min. The solid material was decanted, washed with fresh benzene (toluene for the low temperature grafting), and dried under high vacuum (ca. 10^{–5} mbar) for several hours.

With the use of IR spectroscopy to monitor grafting, a decrease of the isolated silanol band at 3747 cm^{–1} and an appearance of broad bands at 3700–3500 cm^{–1} were observed in all cases; the latter can be associated with remaining silanols interacting with the ligands of the grafted complex. Detection of the corresponding alcohol, silanol, or pyrrole in the washing solution indicates the substitution of the X ligand by a surface siloxy group upon protonolysis with the surface silanol. The amount of HX released during grafting was measured by ¹H NMR with ferrocene as an internal standard, indicating elimination of 0.7–0.9 equiv of HX per initial surface silanol group. Reduced values were observed for OSi(OtBu)₃ complexes, especially for catalysts having a low percentage of grafting (vide infra), likely due to the liberated HOSi(OtBu)₃ that was retained on the surface by strong interactions with the remaining surface silanols.¹³ Typically, siloxide complexes give rise to lower metal content in the sample (2.5–2.7 wt % compared to 3.4–4.1 wt % for other complexes, Table 1), with excess of the unreacted complex being observed in washing solutions by NMR. We associate this behavior mainly with significant steric bulk of this ligand, but also with its propensity to interact strongly with surface silanols.

The structure of all surface complexes was further confirmed with elemental analysis and solid-state NMR spectroscopy (¹H, ¹³C, and ¹⁹F in case of NAr_{F₅} series). The observed W/C/H/N/F ratios (Table 1) and NMR chemical shifts (Supporting

Table 1. Mass Balance and Elemental Analyses of Grafted Complexes

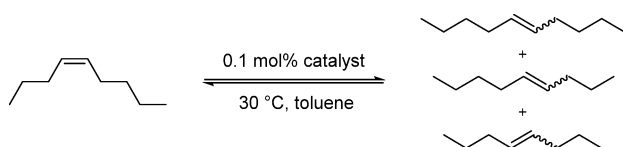
cat.	W, wt % ^a	HX ^b	C/W ^{a,c}	H/W ^{a,c}	N/W ^{a,c}	F/W ^{a,c}
2a	3.87	0.7	20(20)	14(15)	1(1)	9(9)
2b	4.14	0.7	21(20)	19(18)	1(1)	6(6)
2c	2.81	0.6	27(28)	49(42)	2(1)	–
2d ^d	3.90	0.8	20(20)	27(24)	1(1)	–
2e	4.15	0.9	22(22)	23(23)	3(2)	–
3a	3.62	0.8	23(21)	23(16)	1(1)	14(12)
3b	3.90	0.8	22(21)	23(19)	1(1)	9(9)
3c	2.27	0.1	36(29)	63(43)	1(1)	2(3)
3e	3.54	0.9	22(23)	23(24)	2(2)	3(3)
4a ^d	3.46	0.9	23(24)	20(22)	1(1)	13(14)
4b ^d	3.08	0.7	20(20)	17(15)	1(1)	11(11)
4e	4.13	0.9	22(22)	21(20)	2(2)	5(5)

^aAccording to elemental analysis. ^bAmount of HX released per surface silanol group determined by NMR. ^cTheoretical value given in parentheses. ^dGrafting performed at low temperature.

Information) correspond to those expected in accordance with Scheme 2.

A typical side-reaction that is reported to accompany grafting of alkylidene complexes onto silica surface is protonation of the alkylidene ligand by the surface silanol group leading to metathesis-inactive species ($\equiv\text{SiO})\text{W}(\text{NAr})(\text{CH}_2\text{CMe}_2\text{R})\text{X}_2$. Presence of these species can be assessed by the reduced amount of HX released during grafting and increased C, H, F, etc. content in elemental analysis data, but these criteria may be misleading in the case of $\text{OSi}(\text{OtBu})_3$ and other ligands that can remain on the surface (see above). Unfortunately, these species are also difficult to observe by solid-state NMR without using labeled molecular precursors. We have previously observed significant amounts of protonation for $\text{W}(\text{NAr}_{\text{iPr}})(=\text{CHtBu})\text{X}_2$ complexes with the most electron-donating X ligands in the set, namely OtBu and OtBu_{F_3} ,^{4j} as well as for aryloxide complex $\text{W}(\text{O})(=\text{CHCMe}_2\text{Ph})(\text{OHMT})_2$.^{4h} As was shown for OtBu complex **1d'**, the amount of protonated species could be reduced by carrying out grafting at low temperature.^{4j} This approach was successfully applied here to prepare complex **2d**, but preliminary study of grafting of **3d'** and **4d'** showed almost no $t\text{BuOH}$ release and the materials obtained displayed negligible catalytic activity toward olefin metathesis. We associate this behavior with loss of the alkylidene ligand via protonation. Thus, the ability of these complexes to undergo protonation seems to correlate with their instability in solution (see Supporting Information).

Catalytic Activity. All of the grafted catalysts were tested in self-metathesis of *cis*-4-nonene according to the previously established procedure^{4j} (Scheme 3). It should be noted that the performances of olefin metathesis catalysts are strongly affected by the purity of the substrate. All of the data presented was obtained by strictly applying the same conditions of substrate purification and catalyst manipulation and using a single batch of purified *cis*-4-nonene. The tests were repeated multiple

Scheme 3. *cis*-4-Nonene Self-Metathesis

times, affording reproducible results. For the detailed procedures of preparation of *cis*-4-nonene and performing the catalytic tests, see the Supporting Information.

The reaction leads to an equilibrium mixture of *cis/trans* 4-octenes, 4-nonenes, and 5-decenes, corresponding to ca. 50% conversion of nonene. Two measured outputs were typically used to evaluate the catalytic performance: initial TOF measured after 3 min of the reaction and time required to reach equilibrium. No initiation period was observed with any of the catalysts. Thus, the former measure reflects the activity ($\text{TOF}_{3 \text{ min}}$), and the latter is also related to catalyst stability (time to thermodynamic conversion).

Interested in investigating the effect of particular ligand combinations on catalytic activity, we focus our discussion on $\text{TOF}_{3 \text{ min}}$ (Table 2). The detailed catalytic data is found in the

Table 2. Catalytic Activity of Grafted Complexes in Self-Metathesis of *cis*-4-Nonene^a

	NAr_{iPr}	NAr_{Cl}	NAr_{CF_3}	NAr_{F_5}
OtBu	5	45	–	–
Me_2Pyr	9	55	67	81
$\text{OSi}(\text{OtBu})_3$	41	50	59	–
OtBu_{F_6}	75	51	44	38
OtBu_{F_9}	115	49	33	25

^a0.8 M toluene solution, batch reactor, 30 °C, catalyst loading 0.1 mol % W (calc. on the basis of elemental analysis); activity is expressed as initial TOF after 3 min of reaction ($\text{TOF}_{3 \text{ min}}, \text{min}^{-1}$).

Supporting Information. The data presented in Table 2 indicates a bifurcated trend when the entire series of various imido and X ligands is assessed. Within the NAr_{iPr} series, increases in catalytic activity are associated with the enhanced electron-withdrawing character of the X ligand.^{4j} However, the inverse correlation is observed for NAr_{F_5} where decreasing electron-withdrawing ability improves catalytic activity. With NAr_{Cl} and NAr_{CF_3} spanning the transition between these two extreme scenarios, two main trends combining effects of both X and imido ligands on catalytic activity are observed.

- (1) The activity gradually decreases throughout the series with X = OtBu_{F_9} and increases for the series with X = Me_2Pyr when changing from NAr_{iPr} to more electron-withdrawing imido groups.
- (2) While moving across the NAr_{iPr} series, the activity correlates with the electron-withdrawing character of the X ligand, but the opposite trend is observed within the NAr_{CF_3} and NAr_{F_5} series. Catalysts bearing the NAr_{Cl} imido group seem to be an intermediate case; they do not display any pronounced maximum activity within the series.

Overall, these data indicate a cooperative influence of NAr and X ligands on catalytic activity.

Metallacyclobutane Intermediates. Previously, we were able to spectroscopically characterize surface metallacyclobutane intermediates obtained by exposure of grafted tungsten imido–alkylidene complexes **1a–1e** to bis(¹³C-labeled)-ethylene.^{4e,j} Within the NAr_{iPr} series, we found that the ratio between TBP and SP metallacycles (that could be estimated on the basis of ¹³C solid-state NMR spectroscopy) could serve as a measure of σ -donating ability of X ligand, which correlated with the catalytic activity of grafted complexes. Herein, we investigated whether this trend is also observed when changing

the imido ligand. Several grafted complexes of NAr_{Cl} and NAr_{CF_3} series were exposed to bis(^{13}C -labeled)ethylene under the previously reported conditions. TBP/SP ratios of surface metallacyclobutanes were determined from solid-state NMR. The results summarized in Table 3 demonstrate that the imido

Table 3. TBP/SP Ratio of Metallacyclobutanes Obtained by Exposure of Grafted Complexes to ^{13}C -Labeled Ethylene

	NAr_{IPr}	NAr_{Cl}	NAr_{CF_3}
OtBu _{F9}	88/12	86/14	92/8
OtBu _{F6}	67/33	67/33	61/39
OtBu	0/100	0/100	–

ligand in these cases has no influence on the TBP/SP ratio, which was primarily dependent on the nature of the X ligand. Accordingly, with this broader series of catalysts, no direct correlation between TBP/SP ratio and catalytic activity of grafted complex is observed (Tables 2 and 3).

Parameterization. The reversal of TOF trends observed for $\text{X} = \text{Me}_2\text{Pyr}$ as compared to the weaker σ -donating ligand $\text{X} = \text{OtBu}_{\text{F9}}$ (Table 2), along with increasingly electrophilic imido groups, suggests a cooperative effect between the X and NAr moieties in tuning the catalyst activity. To further understand how this cooperative effect impacts the activity (TOF), potentially influencing the design of new tungsten imido–alkylidene metathesis catalysts, we analyzed electronic¹⁴ and steric¹⁵ parameters that were hypothesized to be significant for describing molecular changes to X and NAr. From a panel of the molecular descriptors including IR frequencies and intensities,¹⁴ NBO charges,^{16,17} pK_{a} , proton affinity, and Sterimol¹⁸ values derived from the parent organic molecules, HX and ArNH_2 (Figure 1A), multivariate linear regression analysis was employed to relate these normalized parameters to the TOF of the tungsten imido–alkylidene catalysts. With the use of a training set (red squares, Figure 1B), regression analysis afforded a model composed of two interaction terms: the NBO charge of the ArNH_2 nitrogen ($\text{NBO}_{\text{N,ArNH}_2}$) combined with a steric term, Sterimol B_5 of HX ($\text{B}_{5,\text{HX}}$), and the same NBO charge combined with the pK_{a} of HX ($\text{pK}_{\text{a,HX}}$). Further substantiation of this regression model was provided via external validation (blue squares, Figure 1B, $R^2 = 0.95$, slope = 1.01, intercept = 1.2). As depicted in Figure 1, the model displays accurate and predictive capabilities for estimating the TOF in olefin metathesis reactions involving silica-supported tungsten imido–alkylidene catalysts.

The NBO charge on the ArNH_2 nitrogen, which is obtained through natural population analysis according to Seybold and co-workers, was identified to be one of the most correlative to pK_{a} 's of anilines out of several empirical and quantum chemical methods to assign partial charges.¹⁹ Since the $\text{NBO}_{\text{N,ArNH}_2}$ accounts for the electron density on the ArNH_2 nitrogen through identification of which orbitals were involved in bonding,²⁰ it represents the donating ability of the imido nitrogen toward the tungsten metal center, which then further delocalizes to the alkylidene carbon.²¹ The dipole being established between the tungsten and the alkylidene carbon is stabilized by the electron-withdrawing nature of the X ligand, which can be quantified by the $\text{pK}_{\text{a,HX}}$. Of the catalysts evaluated, the highest TOF was observed for the tungsten imido–alkylidene catalyst **1a**, composed of the more acidic X ligand, OtBu_{F9} ($\text{pK}_{\text{a,HX}} = 4.91$ of the alcohol), in combination with the NAr with the most electron-rich substituent, NAr_{IPr} ,

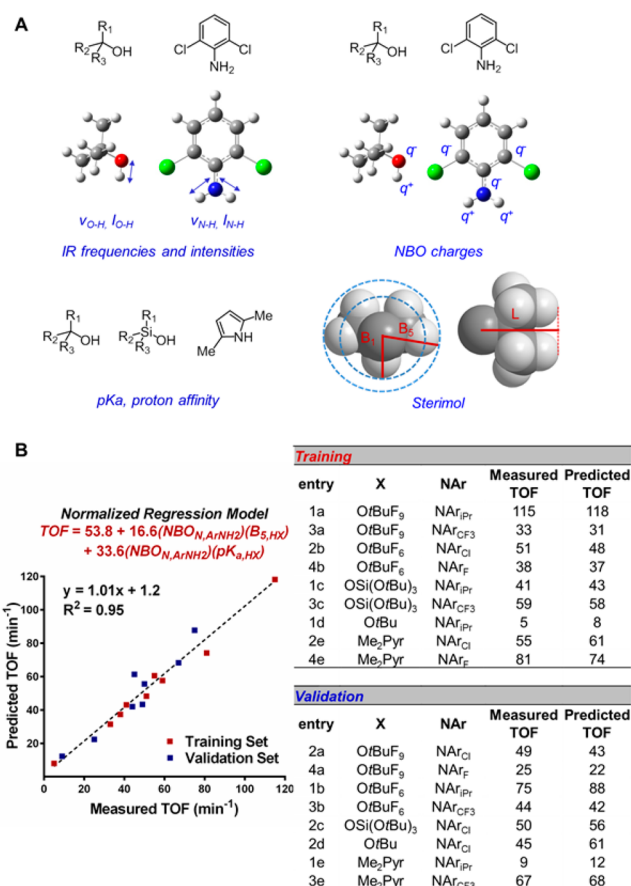


Figure 1. (A) Parameters hypothesized to be significant in quantitatively describing the TOF. (B) Multivariate linear regression model to predict TOF.

($\text{NBO}_{\text{N,ArNH}_2} = -0.811$). While catalyst **4e**, which incorporates the least acidic X ligand, Me₂Pyr ($\text{pK}_{\text{a,HX}} = 17.97$ of the amine), results in its highest TOF when combined with the most electron-poor aryl imido of the series, NAr_{F_5} ($\text{NBO}_{\text{N,ArNH}_2} = -0.779$). Two of the highest TOFs were observed using X and NAr ligand combinations with opposite $\text{NBO}_{\text{N,ArNH}_2}$ and $\text{pK}_{\text{a,HX}}$ values. This is consistent with the inclusion of the interaction term in the model ($\text{NBO}_{\text{N,ArNH}_2})(\text{pK}_{\text{a,HX}})$, which supports the empirical observation of an interplay between the electronic contribution of these ligands that tunes the catalyst and affects the TOF. Furthermore, we also observed that the $\text{NBO}_{\text{N,ArNH}_2}$ measurement correlates well with the intensity of the symmetric N–H stretch, $I_{\text{N-H(s),ArNH}_2}$, a descriptor for changes in dipole moment as well as conjugative effects (see Supporting Information, Figure S44 and S45).

From the obtained regression model, the other interaction term ($\text{NBO}_{\text{N,ArNH}_2})(\text{B}_{5,\text{HX}})$ indicates that the size of the X ligand is also influencing the TOF of the tungsten imido–alkylidene catalyst. For example, the ligands $\text{X} = \text{OSi}(\text{OtBu})_3$ and $\text{X} = \text{Me}_2\text{Pyr}$ resulted in the same increasing TOF trend toward a more electrophilic NAr. However, this increase with the ligand $\text{X} = \text{OSi}(\text{OtBu})_3$ does not result from an increased $\text{pK}_{\text{a,HX}}$ but can be attributed to its large size in terms of Sterimol B_5 .

CONCLUSION

Following the preparation of a wide range of silica-supported tungsten imido–alkylidene metathesis catalysts [(≡SiO)W(=

NAr)(=CHCMe₂R)X] bearing various NAr and X supporting ligands, we studied the catalytic activity of these complexes toward self-metathesis of *cis*-4-nonene as a prototypical olefin substrate and demonstrated a quantitative structure–activity relationship pointing to a cooperative effect between the NAr and X ligands as a push–pull effect. The highest activity within the series was observed for the catalysts bearing NAr and X ligands with opposing electronic properties. This cooperative effect was quantitatively exhibited through multivariate linear regression analysis, which demonstrated that the NBO charge on the nitrogen or the symmetric N–H stretch of ArNH₂, corresponding to the imido ligand, together with the Sterimol B₅ and pK_a of HX, corresponding to the X ligand, mutually contribute to the TOF of these silica-supported tungsten imido–alkylidene catalysts. In other words, the activity (TOF) can be predicted from readily available and easily computed parameters of the parent organic molecule HX and ArNH₂, i.e., the pK_a and Sterimol B₅ of X and the NBO charge on N or the intensity of the symmetric N–H stretch of ArNH₂. Further studies to improve the TOF of these tungsten alkylidene catalyst will be focused on using more electron-rich imido groups as well as expanding the scope on sterically differentiated X ligands. While previous computational studies describe how the steric and electronic nature of the ligands could affect the activity of imido–alkylidene catalysts, this study highlights the synergy and provides a quantitative relationship between the electronic and steric influences of X and NAr and the activity of supported metathesis catalysts, thus paving the way to develop improved catalysts in a more rational way.

■ ASSOCIATED CONTENT

■ Supporting Information

Synthesis and characterization of molecular precursors and grafted complexes, IR and solid-state NMR spectra, catalytic data, and computational details. The Supporting Information is available free of charge on the ACS Publications website at DOI: 10.1021/jacs.5b03344.

■ AUTHOR INFORMATION

Corresponding Authors

*ccoperet@inorg.chem.ethz.ch

*sigman@chem.utah.edu

Author Contributions

[†]These authors contributed equally.

Notes

The authors declare no competing financial interest.

[‡]On leave from A. N. Nesmeyanov Institute of Organoelement Compounds of Russian Academy of Sciences, Vavilov str. 28, 119991 Moscow, Russia.

■ ACKNOWLEDGMENTS

This article is dedicated to the memory of Yves Chauvin. We thank Mr. Maxence Valla for assistance with the solid-state NMR measurements. We acknowledge Dr. Csaba Hegedus and Dr. Levente Ondi for help and discussion with the synthesis of some of the molecular precursors. The Center for High Performance Computing at the University of Utah is gratefully acknowledged. V.M. is supported by a ETH fellowship (cofunded ETH Zürich-Marie Curie action for people, FEL-08 12-2). We also thank the NSF for partial support of this work (CHE-1361296).

■ REFERENCES

- (1) (a) Ivin, K.; Mol, H. In *Olefin Metathesis and Metathesis Polymerization* (2); Ivin, K. J., Mol, J. C., Eds.; Academic Press: London, 1997. (b) Lwin, S.; Wachs, I. E. *ACS Catal.* **2014**, *4*, 2505–2520.
- (2) (a) Herisson, J. L.; Chauvin, Y. *Makromol. Chem.* **1971**, *141*, 161–176. (b) Chauvin, Y. *Angew. Chem., Int. Ed.* **2006**, *45*, 3740–3747.
- (3) (a) Schrock, R. R. *Acc. Chem. Res.* **1979**, *12*, 98–104. (b) Schrock, R. R.; Depue, R. T.; Feldman, J.; Schaverien, C. J.; Dewan, J. C.; Liu, A. H. *J. Am. Chem. Soc.* **1988**, *110*, 1423–1435. (c) Feldman, J.; Schrock, R. R. *Prog. Inorg. Chem.* **1991**, *39*, 1–74. (d) Nguyen, S. T.; Grubbs, R. H.; Ziller, J. W. *J. Am. Chem. Soc.* **1993**, *115*, 9858–9859. (e) Sanford, M. S.; Love, J. A.; Grubbs, R. H. *J. Am. Chem. Soc.* **2001**, *123*, 6543–6554. (f) Wenzel, A. G.; Grubbs, R. H. *J. Am. Chem. Soc.* **2006**, *128*, 16048–16049. (g) Grubbs, R. H. *Angew. Chem., Int. Ed.* **2006**, *45*, 3760–3765. (h) Schrock, R. R. *Angew. Chem., Int. Ed.* **2006**, *45*, 3748–3759. (i) Malcolmson, S. J.; Meek, S. J.; Sattely, E. S.; Schrock, R. R.; Hoveyda, A. H. *Nature* **2008**, *456*, 933–937. (j) Meek, S. J.; O'Brien, R. V.; Lloveria, J.; Schrock, R. R.; Hoveyda, A. H. *Nature* **2011**, *471*, 461–466. (k) Khan, R. K. M.; Torker, S.; Hoveyda, A. H. *J. Am. Chem. Soc.* **2013**, *135*, 10258–10261.
- (4) (a) Chabanas, M.; Baudouin, A.; Copéret, C.; Basset, J. M. *J. Am. Chem. Soc.* **2001**, *123*, 2062–2063. (b) Blanc, F.; Copéret, C.; Thivolle-Cazat, J.; Basset, J. M.; Lesage, A.; Emsley, L.; Sinha, A.; Schrock, R. R. *Angew. Chem., Int. Ed.* **2006**, *45*, 1216–1220. (c) Rhers, B.; Salameh, A.; Baudouin, A.; Quadrelli, E. A.; Taoufik, M.; Copéret, C.; Lefebvre, F.; Basset, J. M.; Solans-Monfort, X.; Eisenstein, O.; Lukens, W. W.; Lopez, L. P. H.; Sinha, A.; Schrock, R. R. *Organometallics* **2006**, *25*, 3554–3557. (d) Blanc, F.; Berthoud, R.; Salameh, A.; Basset, J. M.; Copéret, C.; Singh, R.; Schrock, R. R. *J. Am. Chem. Soc.* **2007**, *129*, 8434–8435. (e) Blanc, F.; Berthoud, R.; Copéret, C.; Lesage, A.; Emsley, L.; Singh, R.; Kreickmann, T.; Schrock, R. R. *Proc. Natl. Acad. Sci. U.S.A.* **2008**, *105*, 12123–12127. (f) Blanc, F.; Rendon, N.; Berthoud, R.; Basset, J. M.; Copéret, C.; Tonzetich, Z. J.; Schrock, R. R. *Dalton Trans.* **2008**, 3156–3158. (g) Rendon, N.; Berthoud, R.; Blanc, F.; Gajan, D.; Maishal, T.; Basset, J. M.; Copéret, C.; Lesage, A.; Emsley, L.; Marinescu, S. C.; Singh, R.; Schrock, R. R. *Chem.—Eur. J.* **2009**, *15*, 5083–5089. (h) Conley, M. P.; Mougél, V.; Peryshkov, D. V.; Forrest, W. P.; Gajan, D.; Lesage, A.; Emsley, L.; Copéret, C.; Schrock, R. R. *J. Am. Chem. Soc.* **2013**, *135*, 19068–19070. (i) Conley, M. P.; Forrest, W. P.; Mougél, V.; Copéret, C.; Schrock, R. R. *Angew. Chem., Int. Ed.* **2014**, 14221–14224. (j) Mougél, V.; Copéret, C. *Chem. Sci.* **2014**, *5*, 2475–2481. (k) Mougél, V.; Pucino, M.; Copéret, C. *Organometallics* **2015**, *34*, 551–554.
- (5) (a) Solans-Monfort, X.; Clot, E.; Copéret, C.; Eisenstein, O. *Organometallics* **2005**, *24*, 1586–1597. (b) Solans-Monfort, X.; Clot, E.; Copéret, C.; Eisenstein, O. *J. Am. Chem. Soc.* **2005**, *127*, 14015–14025. (c) Poater, A.; Solans-Monfort, X.; Clot, E.; Copéret, C.; Eisenstein, O. *J. Am. Chem. Soc.* **2007**, *129*, 8207–8216. (d) Blanc, F.; Basset, J. M.; Copéret, C.; Sinha, A.; Tonzetich, Z. J.; Schrock, R. R.; Solans-Monfort, X.; Clot, E.; Eisenstein, O.; Lesage, A.; Emsley, L. *J. Am. Chem. Soc.* **2008**, *130*, 5886–5900. (e) Leduc, A. M.; Salameh, A.; Soulivong, D.; Chabanas, M.; Basset, J.-M.; Copéret, C.; Solans-Monfort, X.; Clot, E.; Eisenstein, O.; Bohm, V. P.; Roper, M. *J. Am. Chem. Soc.* **2008**, *130*, 6288–6297. (f) Solans-Monfort, X.; Copéret, C.; Eisenstein, O. *J. Am. Chem. Soc.* **2010**, *132*, 7750–7757. (g) Solans-Monfort, X.; Copéret, C.; Eisenstein, O. *Organometallics* **2012**, *31*, 6812–6822.
- (6) (a) Adlhart, C.; Chen, P. *Angew. Chem., Int. Ed.* **2002**, *41*, 4484–4487. (b) Cavallo, L. *J. Am. Chem. Soc.* **2002**, *124*, 8965–8973. (c) Vyboishchikov, S. F.; Bühl, M.; Thiel, W. *Chem.—Eur. J.* **2002**, *8*, 3962–3975. (d) Adlhart, C.; Chen, P. *J. Am. Chem. Soc.* **2004**, *126*, 3496–3510. (e) Correa, A.; Cavallo, L. *J. Am. Chem. Soc.* **2006**, *128*, 13352–13353. (f) Stewart, I. C.; Benitez, D.; O'Leary, D. J.; Tkatchouk, E.; Day, M. W.; Goddard, W. A.; Grubbs, R. H. *J. Am. Chem. Soc.* **2009**, *131*, 1931–1938. (g) Ragone, F.; Poater, A.; Cavallo, L. *J. Am. Chem. Soc.* **2010**, *132*, 4249–4258. (h) Nuñez-Zarur, F.;

Solans-Monfort, X.; Rodríguez-Santiago, L.; Pleixats, R.; Sodupe, M. *Chem.—Eur. J.* **2011**, *17*, 7506–7520. (i) Liu, P.; Xu, X.; Dong, X.; Keitz, B. K.; Herbert, M. B.; Grubbs, R. H.; Houk, K. N. *J. Am. Chem. Soc.* **2012**, *134*, 1464–1467.

(7) Rhers, B.; Quadrelli, E. A.; Baudouin, A.; Taoufik, M.; Copéret, C.; Lefebvre, F.; Basset, J. M.; Fenet, B.; Sinha, A.; Schrock, R. R. *J. Organomet. Chem.* **2006**, *691*, 5448–5455.

(8) (a) Ibrahim, I.; Yu, M.; Schrock, R. R.; Hoveyda, A. H. *J. Am. Chem. Soc.* **2009**, *131*, 3844–3845. (b) Marinescu, S. C.; Levine, D. S.; Zhao, Y.; Schrock, R. R.; Hoveyda, A. H. *J. Am. Chem. Soc.* **2011**, *133*, 11512–11514. (c) Peryshkov, D. V.; Schrock, R. R.; Takase, M. K.; Muller, P.; Hoveyda, A. H. *J. Am. Chem. Soc.* **2011**, *133*, 20754–20757. (d) Reithofer, M. R.; Dobereiner, G. E.; Schrock, R. R.; Muller, P. *Organometallics* **2013**, *32*, 2489–2492.

(9) Wang, C.; Haeffner, F.; Schrock, R. R.; Hoveyda, A. H. *Angew. Chem., Int. Ed.* **2013**, *52*, 1939–1943.

(10) Schrock, R. R.; DePue, R. T.; Feldman, J.; Yap, K. B.; Yang, D. C.; Davis, W. M.; Park, L.; DiMare, M.; Schofield, M. *Organometallics* **1990**, *9*, 2262–2275.

(11) (a) Arndt, S.; Schrock, R. R.; Müller, P. *Organometallics* **2007**, *26*, 1279–1290. (b) Kreckmann, T.; Arndt, S.; Schrock, R. R.; Müller, P. *Organometallics* **2007**, *26*, 5702–5711.

(12) Yuan, J.; Schrock, R. R.; Müller, P.; Axtell, J. C.; Dobereiner, G. E. *Organometallics* **2012**, *31*, 4650–4653.

(13) Héroguel, F.; Siddiqi, G.; Detwiler, M. D.; Zemlyanov, D. Y.; Safonova, O. V.; Copéret, C. *J. Catal.* **2015**, *321*, 81–89.

(14) Milo, A.; Bess, E. N.; Sigman, M. S. *Nature* **2014**, *507*, 210–214.

(15) Harper, K. C.; Bess, E. N.; Sigman, M. S. *Nat. Chem.* **2012**, *4*, 366–374.

(16) (a) Foster, J. P.; Weinhold, F. *J. Am. Chem. Soc.* **1980**, *102*, 7211–7218. (b) Reed, A. E.; Weinstock, R. B.; Weinhold, F. *J. Chem. Phys.* **1985**, *83*, 735–746. (c) Reed, A. E.; Curtiss, L. A.; Weinhold, F. *Chem. Rev.* **1988**, *88*, 899–926.

(17) (a) Glendening, E. D.; Landis, C. R.; Weinhold, F. *WIREs Comput. Mol. Sci.* **2012**, *2*, 1–42. (b) Weinhold, F. *J. Comput. Chem.* **2012**, *33*, 2363–2379.

(18) Verloop, A. *In Drug Design*; Academic Press: New York, 1976; Vol. III.

(19) Gross, K. C.; Seybold, P. G.; Hadad, C. M. *Int. J. Quantum Chem.* **2002**, *90*, 445–458.

(20) *Computational Chemistry Theories and Models*, 2nd ed.; Cramer, C. J., Ed.; The Atrium, Southern Gate: Chichester, England, 2004.

(21) (a) O'Reilly, M. E.; Ghiviriga, I.; Abboud, K. A.; Veige, A. S. *J. Am. Chem. Soc.* **2012**, *134*, 11185–11195. (b) Gonsales, S. A.; Pascualini, M. E.; Ghiviriga, I.; Abboud, K. A.; Veige, A. S. *J. Am. Chem. Soc.* **2015**, *137*, 4840–4845.